Surface Science 225 (1990) 171–183
North-Holland

RECONSTRUCTION AND SUBSURFACE LATTICE DISTORTIONS IN THE (2 × 1)O–Ni(110) STRUCTURE: A LEED ANALYSIS

G. KLEINLE, J. WINTTERLIN, G. ERTL

Fritz-Haber-Institut der Max-Planck-Gesellschaft, D-1000 Berlin 33, Germany

R.J. BEHM, F. JONA * and W. MORITZ

Institut für Kristallographie und Mineralogie, Universität München, D-8000 München 2, Fed. Rep. Germany

Received 9 August 1989; accepted for publication 2 October 1989

LEED analysis of the reconstructed (2 × 1)O–Ni(110) system clearly favors the "missing row" structure over the "saw-tooth" and "buckled row" models. By using a novel computational procedure 8 structural parameters could be refined simultaneously, leading to excellent R-factors ($R_{ZJ} = 0.09$, $R_P = 0.18$). The adsorbed O atoms are located 0.2 Å above the long bridge sites in [001] direction, presumably with a slight displacement (~ 0.1 Å) in [1$\bar{1}$0] direction to an asymmetric adsorption site. The nearest-neighbor Ni–O bond lengths (1.77 Å) are rather short. The separation between the topmost two Ni layers is expanded to 1.30 Å (bulk value 1.25 Å), while that between the second and third layer is slightly contracted to 1.23 Å. The third layer is, in addition, slightly buckled (±0.05 Å). The results are discussed on the basis of our present general knowledge about the structure of adsorbate covered metallic surfaces.

1. Introduction

Despite of considerable efforts structural analyses of reconstructed (metal) surfaces sofar had only limited success, and in many cases results of different experimental techniques are at variance even with respect to the structural model. It has been realized only recently that reconstructions might not be limited to the topmost layer and that deeper reaching distortions of the substrate lattice may play an important role, independent of whether the reconstruction is induced by the bulk truncation at the surface or by the presence of an adsorbate [1–3]. The (2 × 1)O structure on Ni(110) represents a prominent example, where apart from different earlier proposals mainly two reconstruction models, the "missing row" and the "saw tooth" model were advocated in a number of experimental studies [4–10]. In this paper we present results of a LEED structural analysis, which unambiguously identifies this structure as a "missing row" type reconstruction, with significant distortions in the deeper substrate layers. In addition to symmetric vertical and lateral displacements in deeper substrate layers also (asymmetric) lateral displacements of the O_{ad} and the topmost Ni atoms in [1$\bar{1}$0] direction were tested, prompted by the clearcut conclusions of phonon spectroscopy experiments described in the foregoing paper [11]. These rule out the presence of a symmetry plane in [001] direction and accordingly postulate an asymmetric structure as a "saw tooth" structure or a "missing row" structure with an asymmetric adsorption site. We indeed find a slight preference for an asymmetric adsorption site, 0.10 Å off from the long bridge, but the difference in R-factor is so small that a decision between symmetric and asymmetric site could not have been made on the basis of the LEED analysis alone. The results demonstrate the complementary character of the two techniques.

From these data we obtain a detailed picture of the near surface geometry, including the geometry

* Department of Material Science, State University of New York, Stony Brook, NY 11794, USA.

0039-6028/90/$03.50 © Elsevier Science Publishers B.V. (North-Holland)

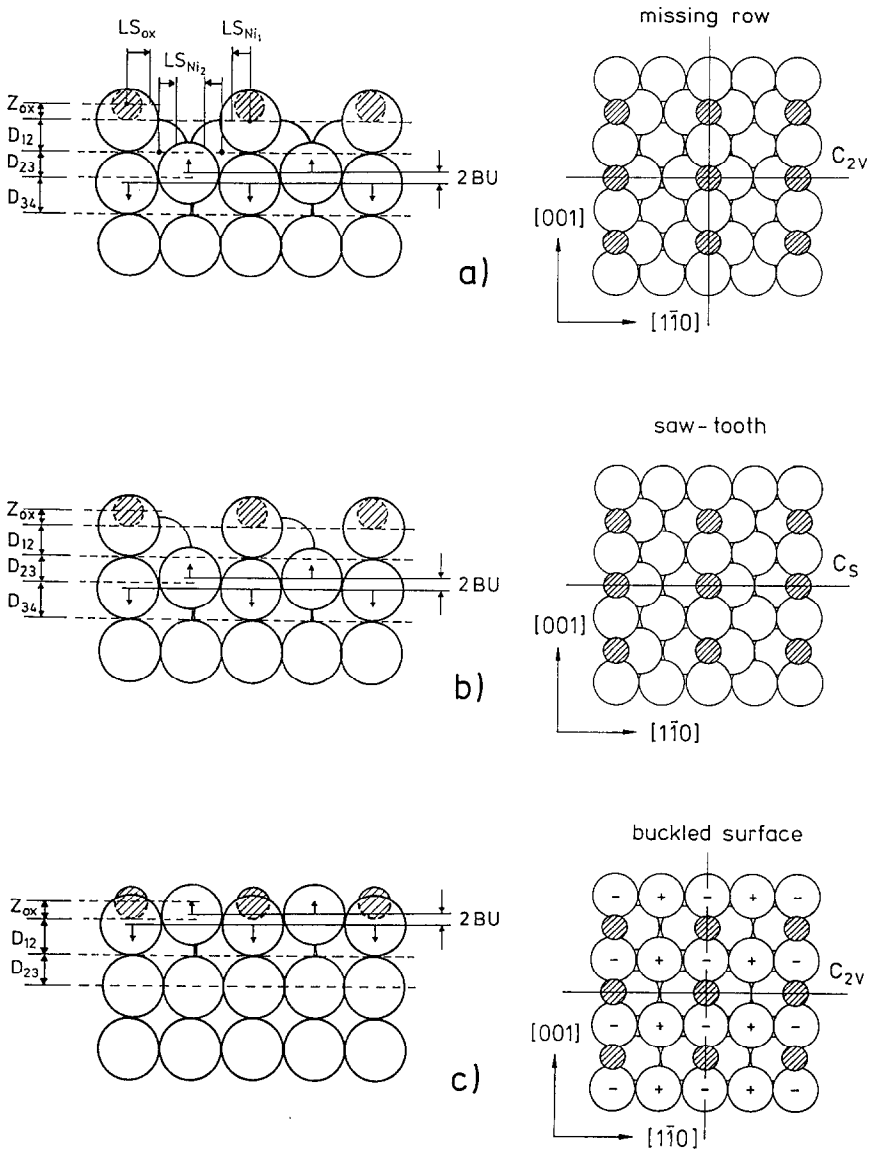

Fig. 1. Structural models (cut along (001) plane left, topview right) and structural parameters varied in this analysis, arrows indicate the shift in the topmost layers with respect to the respective bulk positions. (a) "Missing row" model, (b) "saw-tooth" model and (c) "buckled surface" model.

of the adsorption complex itself and the distortion in the subsurface regime induced by the reconstruction and the presence of the adsorbate. The characteristic features can be rationalized in terms of existing structural and bonding concepts, as discussed below, which can contribute significantly to the current understanding of metal–adsorbate interactions. In addition, the structural outcome bears implications also on the reconstruction mechanism which will be discussed in more detail in a forthcoming paper [12].

Exposure of a clean Ni(110) surface to oxygen at elevated temperatures ($T > 270$ K) leads to a sequence of structures with increasing oxygen

coverage, a (3 × 1), a (2 × 1) and another (3 × 1) structure [6,12,13] at one-third, one-half and two-thirds monolayer coverage, respectively [13]. After annealing the LEED pattern of the (2 × 1) phase is characterized by sharp and intense fractional order spots as first reported by Germer and MacRae [14]. From the high intensity of the extra beams these authors concluded on a reconstruction of the substrate and proposed a model in which every other [001] row of Ni atoms in the topmost layer was replaced by oxygen atoms. Later studies, however, indicated that oxygen atoms are located in the long bridge site along the [001] direction as shown in fig. 1. The "missing row" reconstructed surface of fig. 1a exhibits a deficit of 0.5 monolayers of Ni atoms in the topmost layer, while the "saw tooth" model (fig. 1b) in contrast has no mass deficit and therefore does not require mass transport, in fact it was actually proposed in order to avoid the complications of long range mass transport at relatively low temperatures [15]. The proposal for oxygen chemisorption on the short bridge site along the [1$\bar{1}$0] direction [16] – on an unreconstructed substrate – was found to be inconsistent with Rutherford backscattering [4b], low energy ion recoil spectroscopy [5], and He diffraction [6] data. In an HREELS study Masuda et al. concluded on the existence of two different (2 × 1) structures from the observation of two different loss features upon adsorption at room temperature [17], but there is now convincing evidence that the second loss feature at 480 cm^{-1} relates to the presence of disordered O_{ad} on the non-reconstructed surface, which under those conditions is only partly reconstructed [12]. For a structural analysis of the (2 × 1) ordered surface phase therefore only a single phase had to be considered.

2. Experimental

Details of the experimental setup and procedures can be found elsewhere [12]. Because of the numerous and partly coexisting phases on the oxygen covered Ni(110) surface, exposure and temperature conditions were optimized by LEED and work function measurements to obtain the most perfect (2 × 1) surface. It was formed by exposing the clean Ni(110) surface to 0.80 L (1 L = 1.3×10^{-4} Pa s) at 90 K and subsequent brief annealing to 500 K. The LEED intensity voltage (I–V) spectra were recorded at 90 K – between 40 and 380 eV – by the use of a computer interfaced video system. Normal incidence was verified by a comparison of the spectra from four symmetrically equivalent beams. Correspondingly the final experimental data were obtained by averaging the I–V spectra from beams which are symmetrically equivalent at normal incidence. In total 8 nonequivalent beams, 5 integral- and 3 fractional-order beams were used for the analysis.

3. LEED analysis

Calculations of the LEED intensities were performed by use of the layer-doubling scheme to describe interlayer multiple scattering, the topmost layers including the oxygen atoms were treated as combined layers. Electron scattering at the ion cores was described in the muffin tin approximation, using 9 phase shifts for Ni and 8 for O, respectively. The Ni phase shifts were obtained from a relativistically calculated free atom charge density renormalized by overlapping the contributions from neighboring Ni atoms. These phase shifts were calculated to obtain higher angular momentum components in the extended energy range, they compared very well to a set of phase shift [20] which had been successfully applied in previous LEED intensity calculations for clean and hydrogen covered Ni surfaces [3,18,19]. Oxygen phase shifts were taken from the literature [20] and extensively tested in comparison with other sets. The number of angular momentum components as well as the number of atoms in the unit cell was reduced by the use of symmetry adapted functions [21]. Further nonstructural parameters in the analysis included a constant inner potential, which was initially set to $V_{or} = 10$ eV and then optimized, and an energy dependent imaginary potential $V_{oi} = 0.85(E + V_{or})^{1/3}$. Lattice vibrations were taken into account by a Debye–Waller factor using the bulk Debye temperature of 450 K for all layers. For comparison between

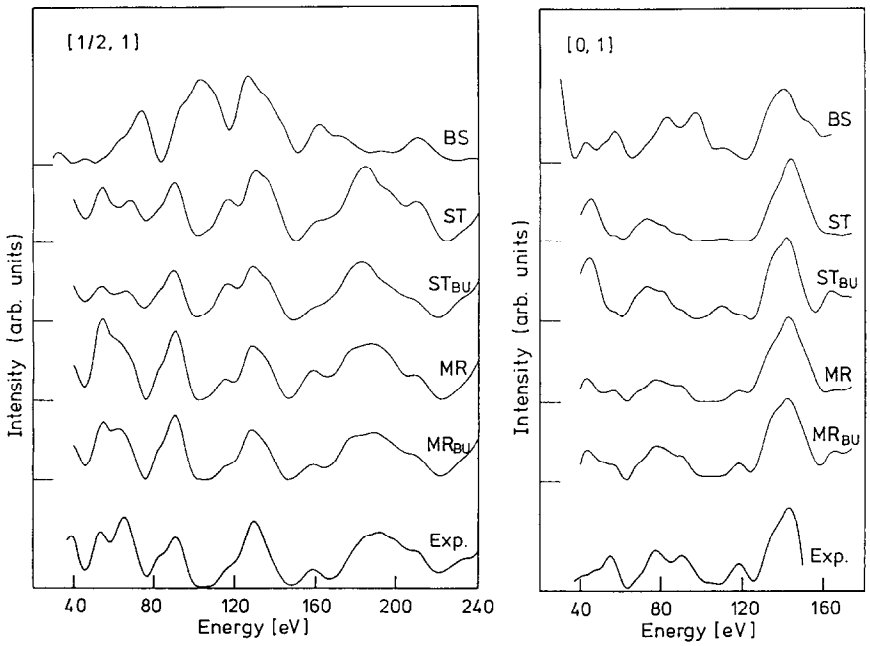

Fig. 2. Comparison of "best fit" calculated and experimental $I-V$ curves for different models, for the ($\frac{1}{2}$, 1)-beam (left panel) and the (0, 1) beam (right panel). Models from top to bottom: BS, ST, ST_{BU}, MR, MR_{BU}, experimental data.

experimental and calculated spectra three different R-factors were used, the Zanazzi–Jona R-factor R_{ZJ} [22], the Pendry R-factor R_P [23] and, in connection with an automatic fit procedure for structural refinement [24], a new R-factor R_{DE}. The latter reflects the mean deviation between calculated and experimental intensities and discrete energies and is defined in analogy to the R-factor used in X-ray diffraction [24]. Part of the analysis was performed by using exclusively this new evaluation scheme, and the full $I-V$ spectra and the other two R-factors were calculated occasionally in addition in order to test the reliability of that method.

Fig. 1 displays the three basic structural models investigated and their respective variable parameters, the "missing row" model (MR), the "sawtooth" model (ST) and the "buckled surface" model (BS). The latter had been proposed for the (2 × 1)O structure on Cu(110) [25]. Based on the convincing evidence from different techniques only the adsorption site on the long bridge in [001] direction was considered for the O_{ad}. On this site the oxygen atom was allowed to reside above or below the topmost Ni layer. In addition to the vertical position of the O_{ad}, Z_{ox}, also the distances D_{12}, D_{23} and D_{34} between the substrate layers marked by their respective indices were varied systematically (fig. 1). For the BS model different degrees and directions of buckling in the topmost layer were tested. For further refinement distortions with the substrate layers were allowed that were compatible with the symmetry of the unit cell and physically reasonable. Following the geometrical trends in the (1 × 2) reconstructed missing row structures of the clean surfaces of the clean surfaces of Pt, Ir and Au [2], a lateral motion $LS_{Ni(2)}$ of Ni atoms in the second layer, in [1$\bar{1}$0] direction, and vertical displacements BU in the third layer, as indicated by the arrows in fig. 1, may be anticipated, in response to the vertical displacement or absence of Ni atoms in the topmost layer. Displacements in both directions were evaluated. Additional vertical displacements in the second layer, which from symmetry arguments should occur only in the ST model, were not

Table 1
R-factors (evaluated for the energy range 40–240 eV in all models) and structural parameters [Å] for the best fit arrangement of the respective structural models

Parameter	as-MR_{BU}	MR_{BU}	MR	ST_{BU}	ST	BS
R_{DE}	0.219	0.229	0.323	0.314	0.378	0.603
R_{ZJ}	0.092	0.095	0.116	0.133	0.167	0.192
R_P	0.176	0.179	0.285	0.424	0.469	0.605
Z_{ox}	0.20	0.20	0.20	0.20	0.16	0.20
D_{12}	1.30	1.30	1.27	1.26	1.29	1.35
D_{23}	1.23	1.23	1.25	1.25	1.25	1.25
D_{34}	1.25	1.25	1.25	1.25	1.25	–
BU	0.05	0.05	–	0.05	–	0.15
LS_{ox}	0.1	–	–	–	–	–
$LS_{Ni(2)}$	0.0	0.0	–	–	–	0.0

as-MR_{BU}: missing row model including third layer buckling and an asymmetric adsorption site for O_{ad}.
MR_{BU}: missing row model including third layer buckling.
MR: missing row model without third layer buckling.
ST_{BU}: sawtooth model including third layer buckling.
ST: sawtooth model without third layer buckling.
BS: buckled surface model including first layer buckling (BU), no third layer buckling.

considered. For the ST model the symmetry is reduced and LEED intensities were averaged over two different domains.

The different structure models were optimized independently, for the MR and ST models sufficient agreement was reached such that the calculated I–V curves reproduce the gross features of the experimental spectra while the agreement for the BS model was poor. A more careful inspection reveals, however, that there are distinct differences in details left. This is demonstrated for two beams, the $(\frac{1}{2}, 1)$ and the (0, 1) beam in fig. 2. Only for the MR model also details are rather well reproduced, and the agreement is further improved by introducing a third layer buckling (which in turn also affected the refinement of the other structural parameters). The kind of agreement for the different models indicated by these beams is typical for the entire set, which is quantitatively reflected by the optimum R-factors for the different structure types.

The optimum lattice parameters and R-factor for the respective models are collected in table 1. This table also indicates the improved agreement introduced by the buckling of the Ni atoms in the third layer, both for the MR and the ST model. From these results the MR model is clearly favored. The resulting R-factors are very low, such degree of agreement so far was achieved only for clean metal surfaces. But note that also for the buckled ST model the R-factors (especially R_{ZJ}) are rather low and reach values that, compared to the other "solved" structures, appear very satisfactory. The simple ST model and the buckled surface model could be excluded from their significantly worse R factors. In all cases the oxygen atoms are positioned slightly above the long bridge site, by ~ 0.2 Å, in good agreement with recent results from ion scattering [4,5,8] and predictions from He diffraction [6].

The sensitivity of the structural analysis is reflected by the variation of the R-factor with modified structural parameters or even a change in the structure model. For the MR model as the best fit model the response of the R_{DE} factor to a change in structural parameters is displayed in figs. 3a–3c.

In each plot two parameters are varied while the other ones are kept constant at or close to their optimum values. From these plots it is evident that the R-factors react very sensitively to all variations in vertical positions, i.e. in the interlayer spacing, in the buckling parameter BU and even in the vertical position of the adsorbed oxygen atoms. Evaluations over an extended range of Z_{ox} (fig. 3c) revealed the existence of additional side minima at 0.9 and 1.6 Å. This result resembles

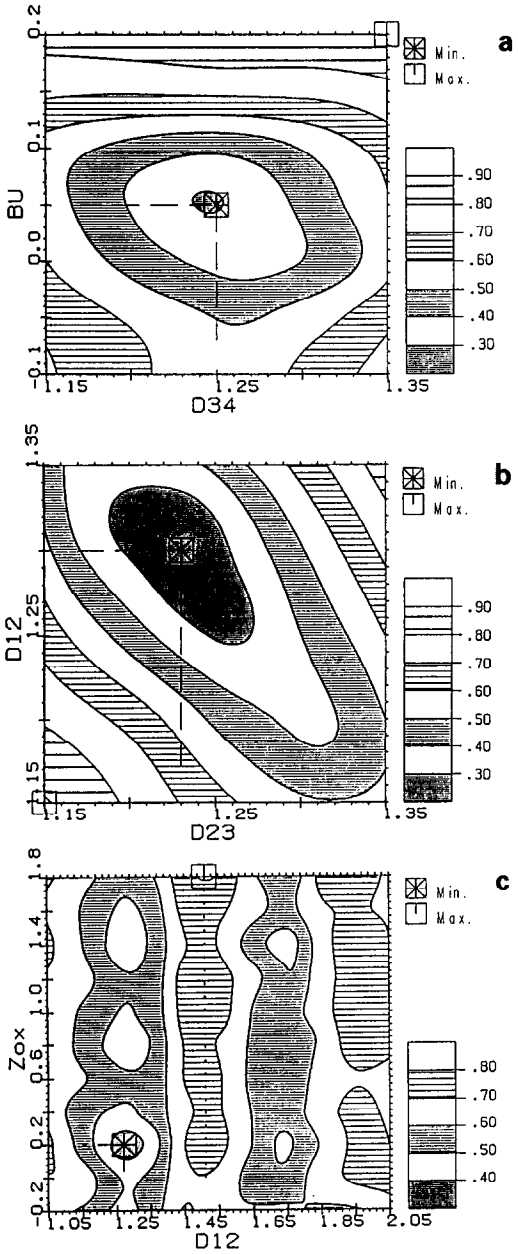

Fig. 3. Contour plots of the R_{DE} factor for the "missing row" model with symmetric adsorption site, two parameters are varied and the remaining ones are kept constant at or close to their optimum values. (a) $R_{DE} = f(D_{34}, \mathrm{BU})$, $D_{12} = 1.25$ Å, $D_{23} = 1.25$ Å, $Z_{Ox} = 0.20$ Å; (b) $R_{DE} = f(D_{12}, D_{23})$, $D_{34} = 1.25$ Å, $Z_{ox} = 0.20$ Å, BU = 0.05 Å; (c) $R_{DE} = f(D_{12}, Z_{ox})$, $D_{23} = 1.25$. Å, $D_{34} = 1.25$ Å, BU = 0.0 Å.

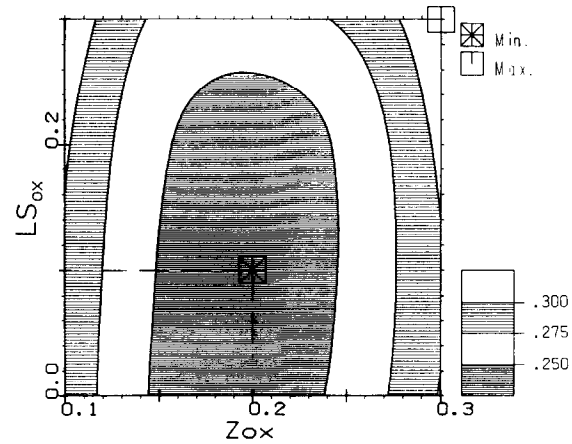

Fig. 4. Contour plot of the R_{DE} factor for variations in the vertical (Z_{ox}) and lateral (LS_{ox}) positions of O_{ad} on the long bridge site of the "best fit" MR model ($D_{12} = 1.30$ Å, $D_{23} = 1.23$ Å, $D_{34} = 1.25$ Å, BU = 0.05 Å).

earlier findings for O/Ni(100) [26] and can be understood in terms of interference effects. Although the sensitivity to lateral positions is significantly lower, lateral displacements LS in the second Ni layer, which would affect two Ni atoms per unit cell, could be ruled out ($LS_{Ni(2)} = 0$).

Stimulated by the afore mentioned results of the HREELS study by Voigtländer et al. [11], which conclusively indicate the absence of a mirror plane in [001] direction, we later extended the parameter space by including an asymmetric adsorption site, with the O_{ad} atom being displaced by LS_{ox} in [1$\bar{1}$0] direction off the long bridge site. In that case also slight shifts of the topmost Ni atoms in [1$\bar{1}$0] direction – $LS_{Ni(1)}$ – were allowed. Because of the clear preference for the MR model and the small effects in the R-factors (see below) by the lateral displacement this site was investigated only for the MR model. As for the ST model, LEED intensities were averaged over two different domains because of the reduced symmetry. The influence of a lateral shift of the O_{ad} on the I–V spectra is very small, up to a shift of $LS_{ox} = 0.3$ Å practically no visible differences can be detected. The R-factor contour plot in fig. 4 describes the response of R_{DE} to variations in the lateral and vertical positions of the adsorbed oxygen, Z_{ox} and LS_{ox}, respectively. There is indeed a minimum in the R-factor plot for an asym-

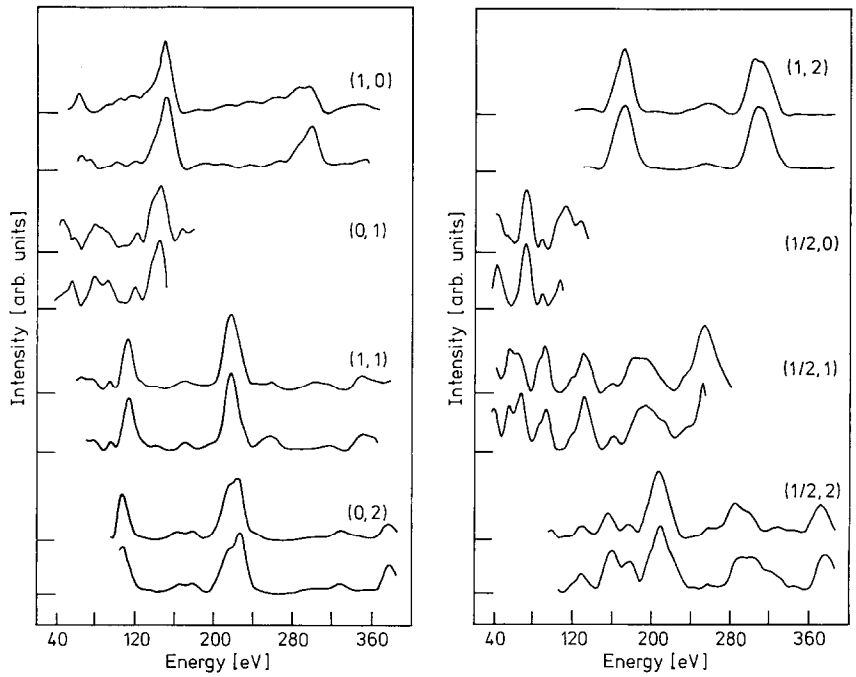

Fig. 5. Calculated (upper) and experimental (lower) I–V spectra for the "best fit" as-MR model.

metric position with $LS_{ox} = 0.10$ Å, which is also found by the automatic fit procedure in good agreement with HREELS results. The optimum vertical position is not affected by the lateral displacement and remains at $Z_{ox} = 0.2$ Å. The decreased sensitivity with respect to lateral displacements found already for $LS_{Ni(2)}$ is here even more pronounced and the minimum in LS_{ox} is very shallow. The difference to the R-factor for the symmetric position, $\Delta R_{DE} = 0.01$ is considered to be within the error limits of this analysis. There was no conclusive evidence for a lateral displacement of the topmost Ni atoms ($LS_{Ni(1)} = 0.0 \pm 0.1$ Å).

After optimising the structure with the novel R_{DE} method including the automatic fit procedure [24] in energy steps of 15 eV (corresponding to 111 data points), a conventional calculation in energy steps of 3 eV was performed for the "best fit" model. The results are presented in fig. 5 together with the experimental I–V curves and demonstrate the quality and reliability of this structural determination.

However, on the basis of the LEED data alone it would not be possible to decide in favor or against the asymmetric adsorption site in the MR model. But in view of the HREELS data [11] we conclude on an asymmetric adsorption site, $LS_{ox} \approx 0.1$ Å, on a buckled MR substrate. The very small changes in R-factors introduced by slight lateral displacements in the topmost layers give an indication of the little improvements to be ex-

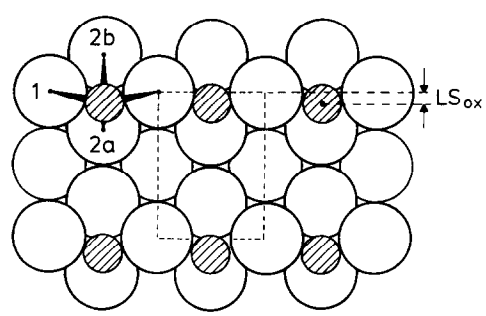

Fig. 6. Top view of the "missing row" reconstructed substrate with an asymmetric adsorption site indicating the local adsorption complex of O_{ad} on (2×1)O-Ni(110) ($r_{Ni(1)-O} = 1.77$ Å (1), $r_{Ni(2)-O} = 1.86$ Å (2a), $r_{Ni(2)-O} = 2.04$ Å (2b)).

pected from similar displacements in the ST and BU model and justify that an asymmetric site was tested only for the by far best structure model, the MR model. For similar reasons no further improvement was to be expected by introducing additional asymmetric displacements in deeper layers.

The geometry of the local adsorption complex becomes obvious from fig. 6. The O_{ad} resides on an asymmetric quasi-threefold site with a bond length $r_{Ni(1)-O} = 1.77$ Å to the nearest neighbor Ni atoms in (001) direction. Although the lateral position of the O_{ad}, LS_{ox}, is less precisely determined than the vertical parameters, this has, for geometric reasons, only very little effect on the *nn* bond distance. Going from the symmetric to the asymmetric site does not change this distance. The n.n.n. distance to the Ni atoms in the second layer in $[1\bar{1}0]$ direction is more affected by the lateral shift of the O_{ad}, it changes from $r_{Ni(2)-O} = 1.95$ Å for the symmetric site to $r_{Ni(2)-O} = 1.86$ Å (2a) and 2.04 Å (2b), respectively, for the asymmetric site.

4. Discussion

The bonding of (atomic) oxygen to Ni surfaces has been a matter of long debate [27]. For O/Ni(100) adsorption on the fourfold hollow site was favored from early on, but different vertical positions for the O_{ad}, ranging from 0.2 to 1.5 Å above the topmost Ni layer and also lateral displacements into an asymmetric site have been proposed [27]. Ab-initio cluster calculations led to two different vertical positions at $Z_{ox} = 0.55$ Å and $Z_{ox} = 0.88$ Å, corresponding to two different states of the adsorbate, the "oxide state" and the "radical state" [28]. Only since recently there appears to be general agreement on a symmetric adsorption site at $Z_{ox} \approx 0.78$ Å [26,29], corresponding to a bond length to n.n. Ni atoms of $r_{Ni(1)} = 1.92$ Å. For Ni(110) the discrepancies went even further, since in addition to the adsorption site also the structure of the substrate remained unclear. For the most frequently investigated (2 × 1) phase a reconstruction of the substrate lattice was proposed already quite early in order to explain the high intensities of the extra beams in the LEED pattern [15]. The authors had put forward a model in which every other row of Ni atoms in [001] directions was replaced by oxygen atoms ("replacement model"). Except for the adsorption site of the O_{ad} this model is identical to the MR model! In a later LEED analysis, however, oxygen adsorption on a short bridge site of the unreconstructed surface was favored [16]. Further studies then agreed on an adsorption site above the long bridge in [001] direction and a reconstruction of the substrate, but the height of the adsorbate and the underlying substrate remained under debate. In the following we will first discuss our results in comparison to previous attempts for a structure determination and then focus on the bonding geometry of the O_{ad} and the distortions of the substrate lattice concomittant to the reconstruction.

The first attempt of a structure determination of this system, the early LEED analysis by Demuth [16], is of little relevance for the present study since it tested different adsorption sites only and did not allow for a reconstruction of the substrate. From He scattering an adsorption site ≈ 0.3 Å above the long bridge was deduced, but the corrugation derived did not allow a clear distinction between MR and ST models [6]. (It should also be noted that this method is not sensitive to deeper lying distortions of the substrate lattice.) A recent NEXAFS study led to similar conclusions [30]. Both low energy ion scattering [4a,8] and Rutherford backscattering [4b] favored the MR model, with O adsorbed in/near the long bridge site [4] or 0.25 Å above this site [8]. In none of these studies, however, interplanar relaxations or intraplanar distortions of the lower substrate layers were considered, and only symmetric adsorption sites were investigated for O_{ad}. From RBS lateral displacements of the Ni atoms by more than 0.1 Å away from the lattice sites could be ruled out [4b], in agreement with the structure determined in the present work.

Structural investigations based on scanning tunneling microscopy (STM) [7], ion induced angular resolved Auger spectroscopy [10] and surface extended X-ray absorption fine structure (SEXAFS) [9] were, in contrast, in favor of the ST

model. With STM, however, it is extremely difficult to conclude the position and even the presence of deeper lying ion cores from the measured line of constant tunnel current [31]. On the other hand, the difference in the Auger yields for the two models were not very pronounced [10], and hence mainly the disagreement with the very conclusive SEXAFS data [9] is left.

The SEXAFS results actually differ from the present findings in two aspects, in the reconstruction model and in the nearest neighbor bond distances to the metal atoms. The preference for the ST model was derived from the ratio of the amplitudes of the adsorption coefficient for different orientations of the electric field vector with respect to the lattice vectors, which depends on the number of backscattering atoms in the respective directions. Agreement with experimental data was significantly better for only one next nearest neighbor in [1$\bar{1}$0], compatible with the ST but not with the MR model. The expected amplitudes, however, were calculated assuming a contraction of the topmost interlayer distance rather than an expansion as found here. The latter would bring the calculated MR amplitudes sufficiently close to the experimental amplitudes ratios to render a decision between the two models impossible. The nearest neighbor distances resulting from the present analysis, $r_{Ni(1)-O} = 1.77$ Å, are significantly smaller than those derived from SEXAFS, $r_{Ni(1)-O} = 1.85$ Å, but in perfect agreement with ion scattering data [5]. This difference is outside the error margins of either study. As already mentioned, the uncertainty in the lateral position of the O_{ad} (and of the topmost Ni-atoms) has only very little influence on the bond distance. The (mean) n.n.n. bond distance $r_{Ni(2)-O} = 1.95$ Å, on the other hand, in contrast agrees well with the value $r_{Ni(2)-O} = 1.96$ Å found from SEXAFS. It should be emphasized that a structure model which combines the present data for the substrate positions and the SEXAFS based bond distances, especially an average distance $r_{Ni(2)-O} = 1.96$ Å, would lead to a very strong lateral displacements ($LS_{ox} = 0.55$ Å and $Z_{ox} = 0.15$ Å) with very different Ni–O distances in [1$\bar{1}$0], 1.61 and 2.31 Å, respectively. The position is not only far outside the error limits of the present study, but would also necessitate an unphysically short Ni–O distance of 1.61 Å. Reduced lateral displacements in turn would demand an increase in the vertical position Z_{ox} which is equally outside the error limits of our results. In conclusion the substrate positions derived here together with the generally accepted height of the O_{ad}, $Z_{ox} = 0.2$–0.3 Å [5,6,8,10], are not compatible with the bond distances derived from SEXAFS. This discrepancy may be related to a specific reason such as the phase shifts used for the SEXAFS analysis which have been modified in a later study [32], but similar effects have been observed in a number of cases and may indicate the existence of more fundamental problems [26].

Adsorption of atomic adsorbates on metal surfaces commonly occurs on highly coordinated sites of the surface, very often corresponding to the lattice sites of an additional substrate layer [33]. Insofar the long bridge site of the O_{ad} on Ni(110) is exceptional. The tendency of the adsorbate atom to a higher coordination is reflected by the lateral displacement of the O_{ad}, but still the n.n. Ni–O bonds in [001] are significantly shorter than the next nearest ones in [1$\bar{1}$0] direction. The short bond length in [001] of 1.77 Å in fact represents the most unusual feature of this adsorption geometry. It is much shorter than the sum of the atomic radius of Ni, 1.246 Å, and the covalent oxygen radius, 0.66 Å [34], respectively. Likewise the Ni–O bond lengths on the other low index Ni surfaces are significantly longer [29,35]. Our result very much resembles recent structural data for O/Cu, where the equally (2 × 1) reconstructed oxygen covered (110) surface exhibits a very short bond distance as well [36,37]. In fact, the shorter bond lengths on (110) planes apparently reflect a general trend, which is demonstrated by several examples in table 2. In all of these cases the n.n. bond distance is significantly shorter on the (110) than on the (100) or (111) surface. For Cl/Ag this effect was associated with a more covalent bond on Ag(110) as compared to the other surfaces [42]. Common feature of all of the X_{ad}–fcc(110) adsorption systems is the relatively low coordination number of the metal atoms the adsorbates are bond to, compared to the close packed (111) and (100) surfaces with coordination numbers of 9 and

Table 2
Nearest neighbor bond distances R_1 [Å] between atomic adsorbates (Ads) and metal substrate atoms (Met) on different low index planes

Met–Ads	(111)	(100)	(110)
Ni–O	1.87 [35]	1.92 [29]	1.77
Cu–O	–	1.90 [38]	1.81 [36] 1.82 [37]
Ag–Cl	2.70 [39]	2.70 [40]	2.56 [41]
Ni–H	1.84 [18]	–	1.72 [19]

8, respectively. The lower coordination numbers are equally found for the unreconstructed and the (2 × 1) missing-row (110) surfaces, in the latter case the effect is even more pronounced. Bonds between these lower coordinated metal surface atoms and the respective atomic adsorbates therefore are expected to exhibit a higher bond order than those on close packed surfaces. As a consequence they are predicted to exhibit significantly shorter bond lengths in accordance with the trends described above. This interpretation agrees well with results of pseudopotential cluster calculations which for smaller Ni_nO clusters find shorter bond lengths [28].

The O_{ad} induced (2 × 1) reconstruction causes distortions in and between deeper lying Ni layers, compared to the clean Ni surface as well as to the bulk arrangement. Such distortions are well known from a number of reconstructions on this and other metal surfaces [1–3,43]. They generally tend (a) to smoothen the corrugation of the surface electronic charge [44] and (b) to reduce bond distortions introduced by the reconstruction of the topmost layer and to gradually adapt to the bulk lattice. This tendency is sketched in fig. 7 for the (1 × 2) "missing row" reconstructed (110) surfaces of Au [2], Ir [45], Pt [46,47] (fig. 7a), the hydrogen covered, (1 × 2) "paired row" reconstructed (110) surfaces of Ni [3] or Pd [43] (fig. 7b) and the present (2 × 1) "missing row" reconstructed, oxygen covered Ni(110) surface (fig. 7c). An overview over lattice distortions different systems is given in table 3.

For the clean (1 × 2) reconstructed surfaces the atoms in the topmost layer move inward in order to reduce the surface charge corrugation. The resulting lattice distortions in the bulk in turn are lowered by the lateral displacements in the second layer ("row pairing") and vertical displacements in the third layer ("buckling") of equal direction, but with a reduced amplitude compared to the first layer. For Pt(110) even a slight row pairing in the fourth layer has been resolved [46]. For the "paired row" (1 × 2) H reconstructions of Ni(110) [3] and Pd(110) [43] the H induced pairing of the topmost layer causes a buckling of the second layer. Recent refinements of these calculations could identify the – expected – decreasing lateral and vertical displacements in the third and fourth layer, respectively [24,49]. The interlayer spacings

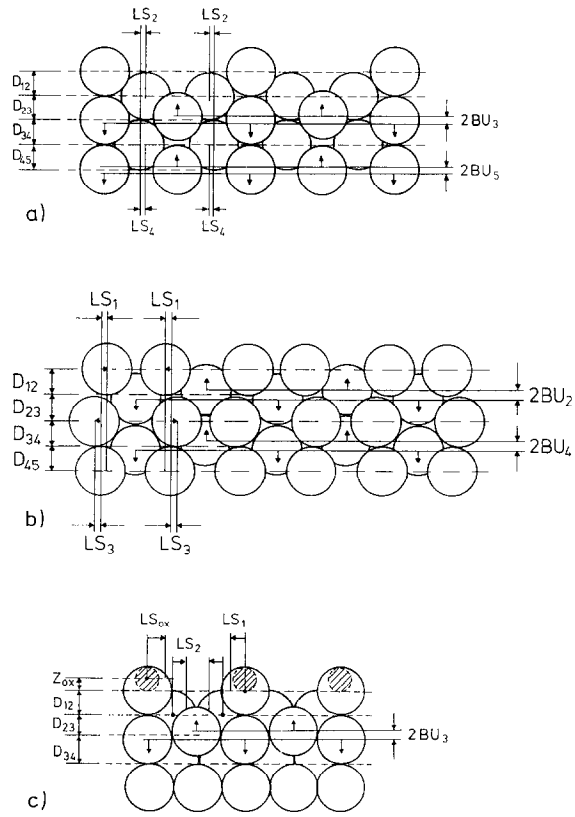

Fig. 7. Structure models of different reconstruction types of fcc (110) surfaces indicating the displacements of surface and subsurface atoms with respect to their respective bulk positions. (a) (1 × 2) missing row reconstruction of clean Au, Ir and Pt(110), cut along (1$\bar{1}$0) plane, (b) (1 × 2) pairing row reconstruction of hydrogen covered Ni(110) and Pd(110), cut along (1$\bar{1}$0), (c) (2 × 1) missing row reconstruction of (2 × 1)O-Ni(110), cut along (001).

Table 3
Lattice parameters and relative deviations from the bulk positions for the best fit "missing row" model with asymmetric adsorption site in comparison to the non-reconstructed clean [19] and the sulfur covered c(2 × 2)S-Ni(110) [48] surface, the hydrogen covered "paired row" reconstructed (1 × 2) H-Ni(110) [24] and the clean, (1 × 2) "missing row" reconstructed Pt(110) [46]

Parameter	Value (Å)	ΔD (% of D_{bulk})				
		(2 × 1)O-Ni(110)	Ni(110)	c(2 × 2)S-Ni(110)	(1 × 2)H-Ni(110)	(1 × 2)-Pt(110)
Z_{ox}	0.2	–	–	–	–	–
LS_{ox}	0.1	–	–	–	–	–
D_{12}	1.30	+4.3	−8.5 ± 1.5	±10.2	−0.5 ± 1.5	+20.8
D_{23}	1.23	−1.2	+3.5 ± 1.5	−3.2	+6.7 ± 1.5	−1
D_{34}	1.25	0	+1.0 ± 1.5	–	+1.9 ± 1.5	−1
LS_1	–	–	–	–	0.30 Å	–
LS_2	0	–	–	–	–	0.04 Å
LS_3	–	–	–	–	0.12 Å	–
LS_4	–	–	–	–	–	0.02 Å
BU_2	–	–	–	–	0.25 Å	–
BU_3	0.05	–	–	–	–	0.17 Å

are slightly different from those of the clean surface [19], but correspond to the trends expected for a hydrogen covered surface [50]: The oscillatory contraction/relaxation of the clean surface induced by the truncation of the bulk [51] is reduced by the presence of the adsorbate, but in this case not completely removed. Following the scheme described for the (1 × 2) MR reconstructed surfaces one could expect for O/Ni(110) an inward motion of the topmost layer Ni atoms, and equally directed but reduced vertical displacement ("buckling") in the third layer and a lateral displacement in the second layer away from the Ni atoms in the topmost layer. None of this is the case, the topmost Ni atoms move outward, and the second layer Ni atoms do, in the limits of our accuracy, not exhibited any lateral shift. These apparent discrepancies can, however, be rationalized as follows: For strongly bound adsorbates such as O_{ad} or S_a it is by now well known that these cannot only reduce but even may lead to a reversal of the initial, oscillatory contraction/relaxation of the surface, i.e. cause an expansion of the topmost interlayer spacing and a contraction of the subsequent one [26,48,50]. The same effect is found for the (2 × 1)O phase on Ni(110). In this case the effect can even be more pronounced since the O_{ad} is bound to two Ni atoms only, which in addition have a reduced coordination shell as compared to the unreconstructed surface or even the close packed (100) or (111) surfaces. This trend agrees well with our results. The absence of any noticeable lateral shift in the second layer, on the other hand, relates to the surface geometry. For the (1 × 2) reconstructions the lateral displacements in the second layer occur in [001] direction, where the metal atoms are not closely packed. From an energetic point of view these displacements are obviously rather facile. In the present case, for the (2 × 1) structure, however, the lateral displacement would have to occur in the close packed $(1\bar{1}0)$ direction. Apparently the resulting compression of the n.n. Ni atoms takes too much energy to lead to a stabilization of the substrate lattice. The buckling of the third layer Ni atoms finally reflects the reduced bond strength of the topmost Ni atoms to the substrate, which is also responsible for the significant expansion of the topmost interlayer distances.

5. Summary

This paper presents results of a multilayer LEED analysis of the reconstructed (2 × 1)O

structure on Ni(110). Application of a novel automatic fit procedure allowed to optimize up to 8 parameters simultaneously, namely the vertical and lateral position of the adsorbate, the topmost 3 interlayer spacings, a vertical displacement within one and lateral displacements within two substrate layers. Among the different structural models investigated, the "missing row", "saw-tooth" and "buckled row" model, there is a clearcut preference for a "missing row" reconstruction with a slight buckling in the third layer (Bu = 0.05 Å). The excellent R-factors of this analysis (R_{ZJ} = 0.095, R_P = 0.179) – comparable to those achieved on simple, clean metal surfaces – basically rule out any other structural model. The O_{ad} is located 0.2 Å above the long bridge site in [001] direction, a slight preference for a lateral displacement of the O_{ad} in [1$\bar{1}$0] LS_{ox} = 0.10 Å is substantiated by and in good agreement with a recent HREELS analysis. The resulting quasi-threefold adsorption site exhibits a very short distance to n.n. Ni atoms of $r_{Ni(1)-O}$ = 1.77 Å, compared to typical values around 1.9 Å in other systems. This bond contraction is shown to be characteristic for atomic adsorbates on fcc (110) surfaces and is related to the lower coordination number of the topmost metal atoms, especially in the case of the (2 × 1) reconstructed surfaces. Thereby the metal–adsorbate bond becomes more molecule-like leading to a bond contraction. The subsurface lattice distortion (outward relaxation in the topmost interlayer spacing D_{12} = 1.30 Å, slight contraction in the second interlayer distance D_{13} = 1.23 Å), which differ in sign from the (1 × 2) reconstruction of clean (110) surfaces, are discussed and interpreted in terms of adsorbate induced variations in the interlayer distances, as they had been found on nonreconstructed, adsorbate covered surfaces: The oscillatory contraction/relaxation of the topmost interlayer spacings induced by the truncation of bulk is reduced or even reversed by the presence of the adsorbate. The absence of lateral displacements in the second layer is caused by the surface geometry, where in contrast to the (1 × 2) reconstructions with their significant lateral displacements such lateral motions are practically impossible due to the close packed arrangement of Ni atoms in [110] direction.

Acknowledgements

Financial support by the Deutsche Forschungsgemeinschaft through SFB 128 in the early stages of this work is gratefully acknowledged. The collaboration with B. Voigtländer, S. Lehwald and H. Ibach on this project (see preceding paper) was initiated by the European Science Foundation Network in Surface Crystallography.

Note added in proof

These results were confirmed by a subsequent analysis of an extensive data set taken at non-normal incidence, which came to similar structural conclusions. Again the asymmetric site for the O_{ad} was favored by a slight margin.

References

[1] K. Müller, Ber. Bunsenges. Phys. Chem. 90 (1986) 184.
[2] W. Moritz and D. Wolf, Surf. Sci. 163 (1985) L655.
[3] G. Kleinle, V. Penka, R.J. Behm, G. Ertl and W. Moritz, Phys. Rev. Lett. 58 (1987) 148.
[4] (a) J.A. van den Berg, L.K. Verhej and D.G. Armour, Surf. Sci. 91 (1980) 218;
(b) R.G. Smeenk, R.M. Tromp and F.W. Saris, Surf. Sci. 107 (1981) 429.
[5] D.J. O'Connor, Surf. Sci. 173 (1986) 593.
[6] T. Engel, K.H. Rieder and I. Batra, Surf. Sci. 148 (1984) 321.
[7] A. Baro, G. Binnig, H. Rohrer, C. Gerber, E. Stoll, A. Baratoff and F. Salvan, Phys. Rev. Letters 52 (1984) 1304.
[8] H. Niehus and G. Comsa, Surf. Sci. 151 (1985) L171.
[9] K. Baberschke, U. Döbler, L. Wenzel, D. Arvanitis, A. Baratoff and K.H. Rieder, Phys. Rev. B 33 (1986) 5910.
[10] M. Schuster and C. Varelas, Surf. Sci. 134 (1983) 195.
[11] B. Voigtländer, S. Lehwald and H. Ibach, Surf. Sci. 225 (1990) 162.
[12] J. Wintterlin, G. Ertl and R.J. Behm, Surf. Sci., in preparation.
[13] P.R. Norton, P.E. Bindner and T.E. Jackman, Surf. Sci. 175 (1986) 313.
[14] L.H. Germer and A.U. MacRae, J. Appl. Phys. 33 (1962) 1923.
[15] S. Ferrer and H.P. Bonzel, Surf. Sci. 119 (1982) 234.
[16] J.E. Demuth and T.N. Rhodin, Surf. Sci. 42 (1974) 261.
[17] S. Masuda, M. Nishijima, Y. Sakisaka and M. Onchi, Phys. Rev. B 25 (1982) 863.
[18] K. Christmann, R.J. Behm, G. Ertl, M.A. Van Hove and W.H. Weinberg, J. Chem. Phys. 70 (1979) 4168.

[19] W. Reimer, O. Penka, M. Skottke, R.J. Behm, G. Ertl and W. Moritz, Surf. Sci. 186 (1987) 45.
[20] S.Y. Tong, A. Maldonado, C.H. Li and M.A. Van Hove, Surf. Sci. 94 (1980) 73.
[21] W. Moritz, J. Phys. C 17 (1984) 353.
[22] E. Zanazzi and F. Jona, Surf. Sci. 60 (1976) 445.
[23] J.B. Pendry, J. Phys. C 13 (1980) 937.
[24] G. Kleinle, W. Moritz, D.L. Adams and G. Ertl, Surf. Sci. 219 (1989) L637; a full account is in preparation.
[25] R. Feidenhans'l and I. Steensgaard, Surf. Sci. 133 (1983) 453;
K.S. Liang, P.H. Fuoss, G.J. Hughes and P. Eisenberger, in: The Structure of Surfaces, Eds. M.A. Van Hove and S.Y. Tong, Vol. 2 of Springer Series in Surface Sciences (Springer, Berlin, 1985).
[26] S.R. Chubb, P.M. Marcus, K. Heinz and K. Müller, Phys. Rev. B, in press.
[27] C.R. Brundle, J.Q. Broughton, in: Chemical Physics of Solid Surfaces and Heterogeneous Catalysis, vol. 5, Eds. D.A. King and D.P. Woodruff (North-Holland, Amsterdam, 1990).
[28] T.H. Upton and W.A. Goddard, Phys. Rev. Letters 46 (1981) 1635.
[29] K. Heinz, K. Müller, J.B. Pendry, W. Oed, H. Lindner, K. Starke and P. de Andres, submitted.
[30] T. Lindner and J. Somers, Phys. Rev. B 37 (1988) 10039.
[31] J. Tersoff and D. Hamann, Phys. Rev. B 31 (1985) 805.
[32] L. Wenzel, D. Arvanitis, W. Daum, H.H. Rotermund, J. Stöhr, K. Baberschke and H. Ibach, Phys. Rev. B 36 (1987) 7689.
[33] M.A. Van Hove, in: The Nature of the Surface Chemical Bond, Eds. G. Ertl and T. Rhodin (Springer, Berlin, 1979).
[34] L. Pauling, The Nature of the Chemical Bond (Cornell University Press, New York, 1960) table 7-2.
[35] T. Narusawa, M.W. Gibson and E. Tornquist, Surf. Sci. 114 (1981) 331.
[36] J. Wever, J. Züter, D. Wolf and W. Moritz, to be published.
[37] M. Bader, A. Puschmann, C. Ocal and J. Haase, Phys. Rev. Lett. 57 (1986) 3273.
[38] U. Döbler, K. Baberschke, J. Stöhr and D.A. Outka, Phys. Rev. B 31 (1985) 2532.
[39] G.A. Lamble, R.S. Brooks, S. Ferrer, D.A. King and D. Normal, Phys. Rev. B 34 (1986) 2875.
[40] G.M. Lamble, R.S. Brooks, J.C. Campuzano and D.A. King, Phys. Rev. B 36 (1987) 1796.
[41] D.J. Holmes, D.R. Batchelor and D.A. King, Surf. Sci. 199 (1988) 476.
[42] D.J. Holmes, D.R. Batchelor and D.A. King, in: Solvay Conference on Surface Science, Ed. F.W. de Wette (Springer, Berlin, 1988).
[43] (a) W. Moritz, R.J. Behm, G. Ertl, G. Kleinle, V. Penka, W. Reimer and M. Skottke, in: The Structure of Surfaces II, Eds. J.F. van der Veen and M.A. Van Hove (Springer, Berlin, 1988);
(b) G. Kleinle, M. Skottke, V. Penka, G. Ertl, R.J. Behm and W. Moritz, Surf. Sci. 189/190 (1988) 177.
[44] V. Heine and L.D. Marks, Surf. Sci. 165 (1986) 65.
[45] C.M. Chan and M.A. Van Hove, Surf. Sci. 171 (1986) 226.
[46] P. Fery, W. Moritz and D. Wolf, Phys. Rev. B 38 (1988) 7275.
[47] P. Fenter and T. Gustafson, Phys. Rev. B 38 (1988) 10197.
[48] R. Baudoing, Y. Gauthier and Y. Joly, J. Phys. C 18 (1985) 4061.
[49] G. Kleine, PhD Thesis, FU Berlin, 1989.
[50] R.J. Behm, Habilitation, Universität München, 1987.
[51] P. Jiang, F. Jona and P.M. Marcus, Solid State Commun. 59 (1986) 275.